Influence of Al_2O_3 Particles Weight Fraction on Fracture Mechanism of AZ61 Mg-Al_2O_3 System Studied by *In Situ* Tensile Test in SEM

M. Besterci[a], Š. Nagy[b,c], S.-J. Huang[d], O. Velgosová[e,*], K. Sülleiová[a] and P.-C. Lin[d]

[a]Institute of Materials Research, Slovak Academy of Sciences, Watsonova 47, 040 01 Košice, Slovakia

[b]Institute of Materials and Machine Mechanics, Slovak Academy of Sciences, Račianska 75, 831 02 Bratislava, Slovakia

[c]Institute of Materials Science, Faculty of Material Sciences and Technology in Trnava, Slovak University of Technology in Bratislava, Slovakia

[d]National Taiwan University of Science and Technology, Department of Mechanical Engineering, 43, Sec. 4, Keelung Rd., 106 Taipei, Taiwan, R.O.C.

[e]Department of Materials Science, Faculty of Metallurgy, Technical University in Košice, Park Komenského 11, 042 00 Košice, Slovakia

(Received April 16, 2015; in final form July 21, 2015)

In situ observation of AZ61 Mg alloy with 1 and 5 wt% of Al_2O_3 in the scanning electron microscopy was performed to study influence of the weight fraction of Al_2O_3 particles on the deformation and fracture mechanism during tensile test. Structure of the experimental materials was also analysed; microstructures were heterogeneous, with randomly distributed globular Al_2O_3 particles (average diameter of 25 nm) and $Mg_{17}Al_{12}$ intermetallic phase (average diameter of 0.4 μm). It was shown that during tensile deformation the failure of $Mg_{17}Al_{12}$ particles and decohesion of the matrix-Al_2O_3 particles interphase boundary started simultaneously. Decohesion resulted from the different physical properties of matrix and Al_2O_3 particles. The influence of the Al_2O_3 weight fraction on the final fracture was evident; for material with 5 wt% of Al_2O_3, the fracture surface was approximately perpendicular to the loading direction and for material with 1 wt% of Al_2O_3 was at 45° angle. Fracture surface had transcrystalline ductile character.

DOI: 10.12693/APhysPolA.129.138

PACS: 81.05.–t, 62.20.mm, 62.23.Pq

1. Introduction

Magnesium alloys are becoming increasingly attractive for use as structural materials in the automotive industry, primarily because of their low densities, excellent damping capacities and their very good recycling capabilities [1, 2]. Nevertheless, there are some practical limitations on the use of magnesium alloys in industrial applications because of their susceptibility to corrosion and because these alloys are inherently brittle due to their hexagonal crystal structure and the consequent limited number of active slip systems [3–6]. An important current requirement is therefore to develop procedures having the potential for improving the ductility of Mg-based alloys. Now it is well established that the processing of fcc metals through the use of equal-channel angular pressing (ECAP) leads to ultrafine grain sizes that are typically within the submicrometer range [7–10]. In recent years a lot of works deal with metal matrix composites (MMCs) [11–16]. An overview of models for the different material systems is listed in [17].

*corresponding author; e-mail: oksana.velgosova@tuke.sk

The aim of the present study was to analyse the structures of AZ61 Mg alloy and to evaluate the influence of the weight fraction of Al_2O_3 particles (1 and 5 wt%) on the deformation and fracture mechanism.

2. Experimental materials and methods

The matrix used in this work was magnesium alloy AZ61 with ≈6.0% aluminium and ≈1.0% zinc made by Metaltech Industrial Co, LTD, Taiwan. Its chemical composition is shown in Table. During preparation of magnesium alloy, the precipitation of $Mg_{17}Al_{12}$ intermetallic phase occurred [18–20]. Al_2O_3 particles with the weight fractions of 1 and 5% were used as the reinforcement phase. The commercially available Al_2O_3 powder with a particles diameter of about 25 nm, with purity of 99.8%, was added into AZ61 to form Mg-based metal–matrix composites.

TABLE

Chemical composition of AZ61.

Elements	Al	Zn	Mn	Si	Fe	Cu	Ni	Mg
[wt%]	5.83	0.794	0.549	0.013	0.005	0.01	0.008	balance

The melt-stirring technique was used to fabricate the present Mg MMCs. Experimental setup is shown in Fig. 1 [21].

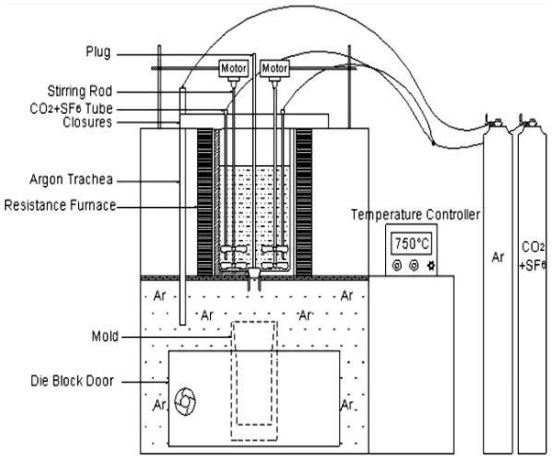

Fig. 1. The melt-stirring scheme used to fabricate the Mg MMCs.

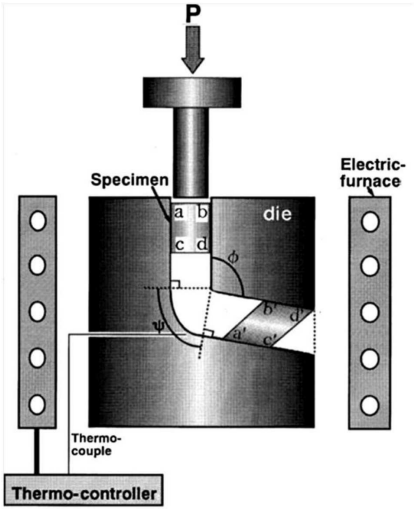

Fig. 2. Scheme of equal-channel angular pressing (ECAP).

The AZ61 was melted at 760 °C in a resistance-heated furnace. Preheated Al_2O_3 particles were simultaneously added to the stirred alloy. The composite melts with different weight fractions of Al_2O_3 (1 and 5 wt%) were poured into a metallic moulds. The AZ61 MMCs were homogenized at 400 °C for 20 h and water quenched, hot extruded by an extrusion ratio of 12.25:1 on a 500 ton hydraulic press. Extrusion was carried out at 300 °C. The preforms were held at 300 °C for 90 min in a constant temperature furnace before extrusion. Bars of $11.0 \times 11.0 \times 90$ mm were processed from the AZ61 and AZ61 MMCs' rods. The scheme of ECAP shown in Fig. 2 was carried out in a die with the die angle $\Phi = 120°$ and the outer die angle $\Psi = 0°$. The extrusion temperature was set at 300 ± 5 °C. During deformation, the plunger speed was about 1.0 mm/s. After each extrusion pass, the billet was quenched into water. The billets were rotated counterclockwise about the exit extrusion axis by 90° between each pass, the so-called Bc route, and each bar was ECAPed by 4 passes.

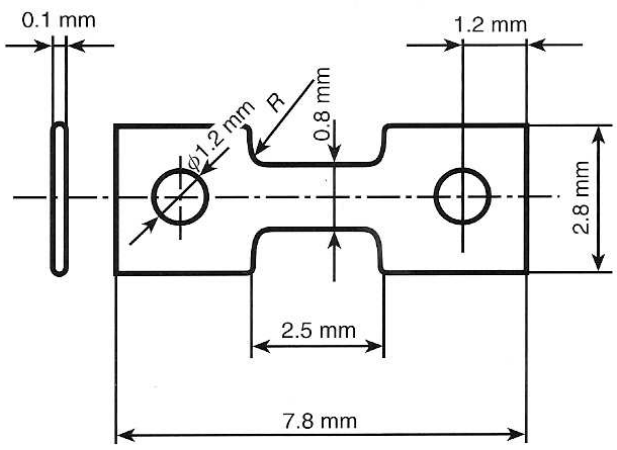

Fig. 3. Tensile test specimen.

Small flat tensile test pieces with 0.1 mm thickness were prepared by electroerosive machining (keeping the loading direction identical to the direction of extrusion), grounded and polished by ion gunning, Fig. 3. The test pieces were fitted into special deformation grips in the JEM 100 C electron microscope, which enables direct observation and measurement of the deformation by the ASID-4D optional instrumentation. Direct observations of the test pieces deformation and failure processes enabled to record the first crack initiation and its propagation.

3. Results and discussion

Microstructure of the experimental materials was heterogeneous. The relation between structural parameters l (distance between rows of particles) and h (the density of particles distributed in rows) can be characterised as follows: $l_{1\ wt\%} > l_{5\ wt\%}$ or $h_{1\ wt\%} > h_{5\ wt\%}$, respectively. Fine Al_2O_3 particles were distributed in rows individually as well as in clusters. The mean size of Al_2O_3 phase particles in both weight fractions was approximately 25 nm, Fig. 4. It was found that with the increasing content of the Al_2O_3 phase, the amount of clusters in the microstructure increased.

Transmission electron microscopy and selective electron diffraction confirmed presence of $Mg_{17}Al_{12}$ phase. This phase has a body centred cubic structure, with the lattice parameter $a = 10.543$ Å and a spherical morphology; particles size was in the range 0.2–0.6 μm and were coherent with the matrix. Based on the microstructural analyses of experimental materials it can be concluded that the weight fraction of the strengthening phase has no significant influence on the sizes of the both Al_2O_3 and $Mg_{17}Al_{12}$ phases.

The matrix was pure Mg with hexagonal close packed lattice, the lattice parameters: $a = 3.21$ Å and $c = 5.21$ Å. In our previous work [22] it was shown that the mean grain size varied from 3.2 μm to 1.5 μm and 0.8 μm for 1, 2 and 5 wt% of Al_2O_3, respectively. The mean grain sizes of MMCs decreased with

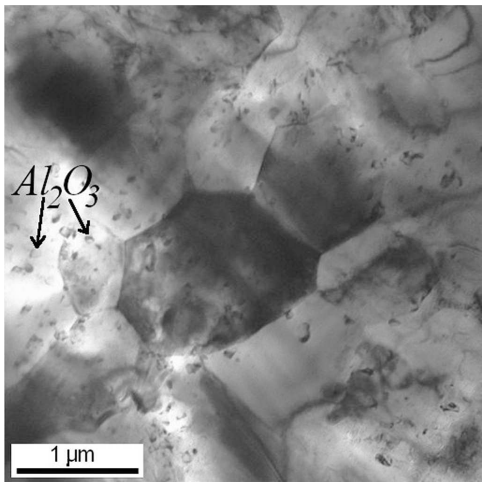

Fig. 4. TEM — distribution of Al_2O_3 particles.

the increasing weight percentages of Al_2O_3 particles [21–23], the nanoparticles act as hard restrictive obstacles against grain growth. The addition of Al_2O_3 nanoparticles not only refined the grain structure but according to Habibnejad–Korayem et al. [23] it decreased the coefficient of thermal expansion.

Samples of experimental materials were deformed at 20 °C at a rate of 6.6×10^{-4} s^{-1} in elastic region. Because the materials have low plasticity due to the presence of $Mg_{17}Al_{12}$ and Al_2O_3 phases, the damage and cracking of the test piece was very fast and depended on the amount and distribution of the particles.

For the composite with 1 wt% of Al_2O_3 cracks were formed by failure of $Mg_{17}Al_{12}$ particles together with decohesion of the matrix-Al_2O_3 particle boundary and Al_2O_3 particle clusters. Further increase of load led to the development of fracture by coalescence of incurred micro failures. The final rupture took place in direction along the 45° angle with respect to the loading; it corresponds to the maximum of share stresses. The fracture was transcrystalline ductile. These results confirmed the conclusions published in the work [22], where the failure mechanism of AZ61-F Mg alloy with 1 wt% of nano-Al_2O_3 particles was studied.

Scanning electron microscopy (SEM) observations of materials with 5 wt% of nano-Al_2O_3 particles showed that during the deformation the cracking of larger ($Mg_{17}Al_{12}$) particles and decohesion at interphase boundaries of smaller ones (Al_2O_3) started simultaneously, Fig. 5. Fracture initiated inside the material and at the sample surface; depending on the distribution of the particles in material. The final fracture surface was perpendicular to the loading direction.

Decohesion is a result of different physical properties of both phases of the system. The Mg matrix has significantly higher thermal expansion coefficient and lower elastic modulus (26.5×10^{-6} K^{-1}, and 44.7 GPa) than Al_2O_3 (8.3×10^{-6} K^{-1}, and 393 GPa) [24]. Big differences in the thermal expansion coefficients α resulted in high stress gradients, which arise on the interphase boundaries during the system preparation. Since $\alpha_{\text{matrix}} > \alpha_{\text{particle}}$, high compressive stresses can be expected. However, the stress gradients arise due to temperature changes, during cooling (which results in increase of the stress peaks) their partial relaxation can occur. Superposition of the external load and the internal stresses can initiate cracking at interphase boundary [3].

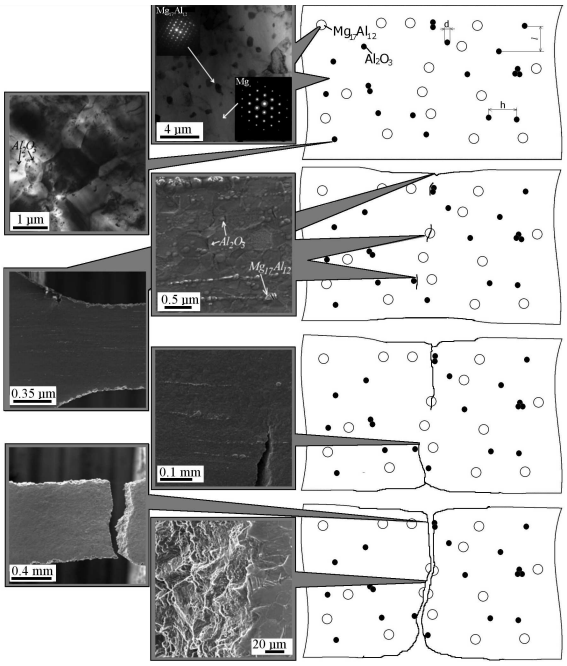

Fig. 5. Model of the fracture mechanism for high wt% of Al_2O_3.

Based on the microstructure changes observed in the process of deformation, the following fracture damage mechanism has been proposed, Fig. 5:

1. The microstructure in the initial state is characterized by Mg matrix, $Mg_{17}Al_{12}$ particles and Al_2O_3 particles (1, 2 and 5 wt%) with geometrical parameters (l, h and d). Fine Al_2O_3 particles are incorporated in the microstructure. Intermetallic $Mg_{17}Al_{12}$ particles have roughly Poisson distribution.

2. Deformation was realized through the slip systems, which mutually interacted by forming of microcracks. During the deformation, failure of $Mg_{17}Al_{12}$ particles occurs and at the same time decohesion of Al_2O_3 dispersoids takes place. Fracture is initiated at the sample surface. Further increase of load leads to the crack growth by coalescence of cavities in the direction from the surface to the specimen centre.

3. The final fracture results from coalescence of the failure formed by decohesion and cracking of the particles inside the material (fractured $Mg_{17}Al_{12}$ particles and, decohesively dislodged dispersed

Al_2O_3 particles) and the crack formed at the edge of the sample.

4. The fracture propagates approximately perpendicularly to the loading direction. The secondary phases lead to transcrystalline ductile comb like fracture with the dimples.

4. Conclusions

Microstructural parameters of the AZ61 Mg system with 1 and 5 wt% of Al_2O_3, namely the matrix grain size and mean size of the dispersed particles were evaluated. Based on the microstructural changes observed during the deformation process, the fracture mechanism for higher wt% of Al_2O_3 has been proposed.

The weight fraction of Al_2O_3 influenced the fracture kinetics. During the deformation, failure of $Mg_{17}Al_{12}$ particles occurred and simultaneously decohesion of Al_2O_3 dispersoids took place. Further increase of load led to the crack growth by coalescence of cavities. The fracture mechanism was identical for 1 and 5 wt% of Al_2O_3 particles. Differences were found only in trajectory of fracture.

Acknowledgments

The work was supported by the Slovak National Grant Agency under the Project VEGA 2/0118/14.

References

[1] A. El-Morsy, A. Ismail, M. Waly, *Mater. Sci. Eng. A* **486**, 528 (2008).

[2] R.M. Wang, A. Eliezer, E.M. Gutman, *Mater. Sci. Eng. A* **344**, 279 (2003).

[3] P. Lukáč, Z. Trojanová, *Kovove Mater.* **44**, 243 (2006).

[4] S.J. Huang, C.R. Li, K.L. Yan, *Kovove Mater.* **51**, 45 (2013).

[5] J.Y. Choi, W.J. Kim, *J. Alloys Comp.* **614**, 49 (2014).

[6] Po-Chou Lin, S.J. Huang, P.S. Hong, *Acta Metall. Slov.* **16**, 237 (2010).

[7] Y. Iwahashi, Z. Horita, M. Nemoto, T.G. Langdon, *Acta Mater.* **45**, 4733 (1997).

[8] Y. Iwahashi, Z. Horita, M. Nemoto, T.G. Langdon, *Acta Mater.* **46**, 3317 (1998).

[9] R.Z. Valiev, T.G Langdon, *Prog. Mater. Sci.* **51**, 881 (2006).

[10] R.Z. Valiev, R.K. Islamgaliev, I.V. Alexandrov, *Prog. Mater. Sci.* **45**, 103 (2000).

[11] M. Besterci, J. Ivan, *J. Mater. Sci. Lett.* **15**, 2071 (1996).

[12] M. Besterci, J. Ivan, *J. Mater. Sci. Lett.* **17**, 773 (1998).

[13] M. Besterci, J. Ivan, L. Kováč, *Mater. Lett.* **46**, 181 (2000).

[14] M. Besterci, J. Ivan, L. Kováč, T. Weissgaerber, C. Sauer, *Mater. Lett.* **38**, 270 (1999).

[15] A. Mocellin, F. Fougerest, P.F. Gobin, *J. Mater. Sci.* **28**, 4855 (1993).

[16] L.V. Broutman, R.H. Krock, *Compos. Mater.* **5**, 27 (1974).

[17] O. Velgosová, M. Besterci, J. Ivan, K. Sülleiová, *Int. J. Mater. Prod. Technol.* **49**, 129 (2014).

[18] M.X. Zhang, P.M. Kelly, *Scr. Mater.* **48**, 647 (2003).

[19] C.J. Bettles, *Mater. Sci. Eng. A* **348**, 280 (2003).

[20] R.M. Wang, A.E.M. Eliezer, I. Gutman, *Mater. Sci. Eng. A* **355**, 201 (2003).

[21] S.J. Huang, P.C.I. Lin, *Kovove Mater.* **51**, 357 (2013).

[22] M. Besterci, J. Ivan, S.J. Huang, O. Velgosová, B.Z. Lin, P. Hvizdoš, *Kovove Mater.* **49**, 451 (2011).

[23] M. Habibnejad-Korayem, R. Mahmudi, W.J. Poole, *Mater. Sci. Eng. A* **519**, 198 (2009).

[24] E.A. Brandes, G.B. Brook, in: *Smithells Metals Reference Book*, Eds.: E.A. Brandes, G.B. Brook, 7th ed., Butterworth-Heinemann, Oxford; Boston 1998.